Determination of NMR Solution Structure of a Branched Nucleic Acid from Residual Dipolar Couplings using Isotope Labeled Nucleotides

Bernd N.M. van Buuren, Jürgen Schleucher, Valentin Wittmann, Christian Griesinger, Harald Schwalbe, Sybren S. Wijmenga [*]

[*] Prof. Dr. Sybren Wijmenga, Laboratory of Physical Chemistry-Biophysical Chemistry, University of Nijmegen, Toernooiveld 1, 6225ED Nijmegen, The Netherlands; Fax: +31-24-3652112; email:sybrenw@sci.kun.nl; Prof. Dr. Harald Schwalbe, Johann Wolfgang Goethe-Universität Frankfurt/M., Zentrum für Biomolekulare Magnetische Resonanz, Institut für Organische Chemie und Chemische Biologie, Marie-Curie-Str. 11, 60439 Frankfurt/M., Germany, Fax.: 0049 69 7982 9515; email:schwalbe@nmr.uni-frankfurt.de; Dr. Bernd N.M. van Buuren, Unilever Research & Development, Olivier van Noortlaan 120, 3133AT Vlaardingen, The Netherlands; Dr. Jürgen Schleucher, Department of Medical Biochemistry and Biophysics, Umeå University, S-90187 Umeå, Sweden; Dr. Valentin Wittmann, Johann Wolfgang Goethe-Universität Frankfurt/M., Institut für Organische Chemie und Chemische Biologie, Marie-Curie-Str. 11, 60439 Frankfurt/M; Prof. Dr. Christian Griesinger, Max-Planck-Institute for Biophysical Chemistry, Am Fassberg 11, D-37077 Göttingen, Germany.

Fig. S1 Correlation between calculated and experimental D_{CH}

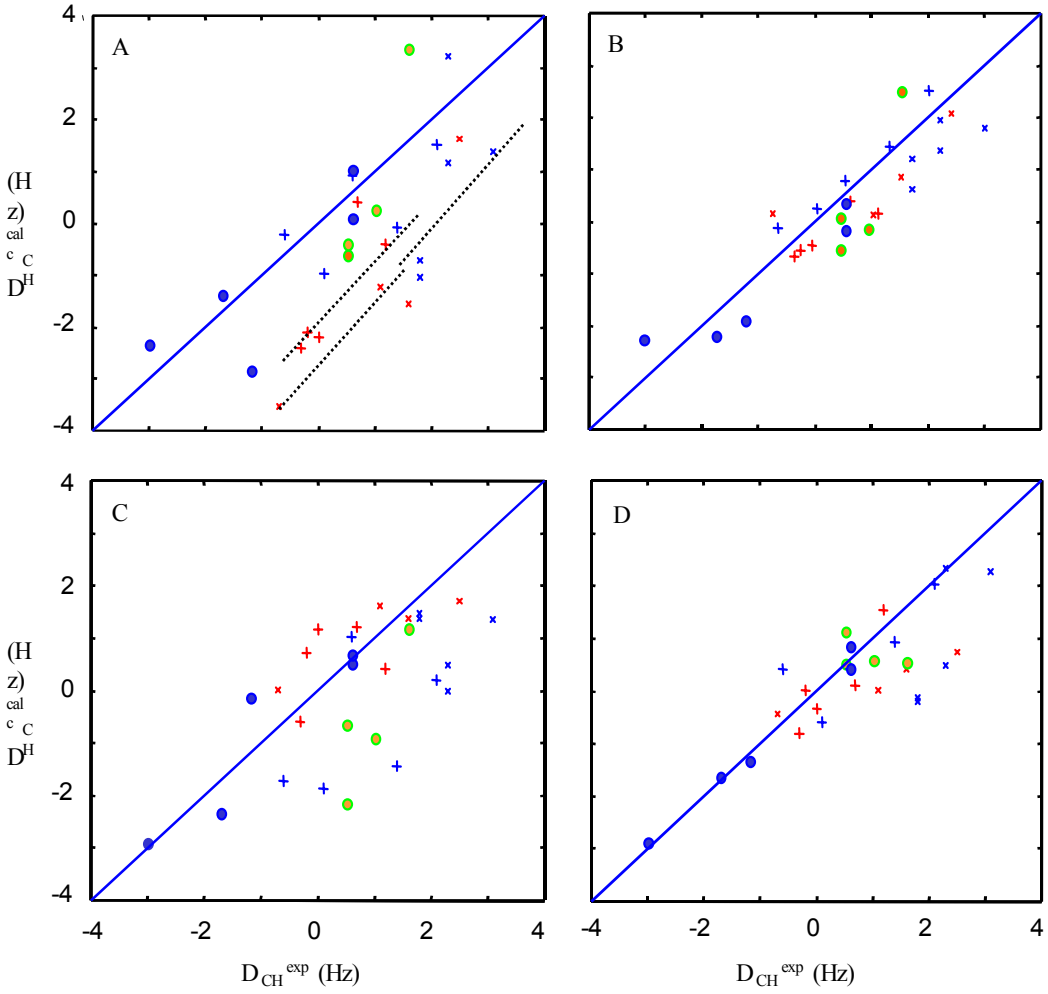

Fig. S1. Correlation between calculated and experimental mRDCs (D_{CH}^{calc} and D_{CH}^{exp}) after different optimizations of the global 4H structure. **A)** Model helices used and optimization with three parameters (ψ, ω_{AD} and ω_{BC}), corresponding to fit M(3)_r1 in Table S1a. Filled blue: C1'-H1' of A- and D -helix; filled red/green: C1'-H1' of B- and C-helix; red plus: C3'-H3' of A and D-helix; blue plus: C4'-H4' of A- and D-helix; red x: C3'-H3' of B- and C-helix; blue x: C4'-H4' of B- and C-helix. Note the offset of the H3'-C3' couplings of the A- and D-helix (red plus) from the diagonal (dotted line is through H3'-C3' of helix AD and indicates the correlation between experimental and calculated couplings). Similar correlated offsets can be seen for the H3'-C3' of the B-and C-helices and for the H4'-C4' of the B- and C-helices. Table S1b gives the required additional group-wise ω-rotation to obtain optimal correlation for these vectors. **B)** As in A except additional group-wise optimization of H3'-C3' and H4'-C4' vectors (fit M(10)_r2 of Table S1a). **C**) Experimental helix used with three-parameter optimization (color coding as in A; fit E2(3)_b1 in Table S1a). **D)** Experimental helices are used and with additional group-wise optimization of H3'-C3' vectors (fit E2(11)_b2 in Table S1a; color coding as in A).

Table S1a Fitting results

Fit[a]	Rmsd[b] (Hz)	R[c]	Q[c]	ψ(°) Helix-angle[d]	ω_{AD} (°)[d]	ω_{BC} (°)[d]	χ_{ax} (Hz)[e]	R_χ[e]	α (°)[f]	β(°)[f]	γ (°)[f]
M(3)_r1	1.51	0.73	0.99	-92(6)	-157(10)	-175(7)	-3.4	-0.76	5	2	7
M(10)_r2[h]	0.69	0.89	0.21	-96(3)	-171(8)	-183(4)	-3.5	-0.70	-4	7	-2
M(12)[h,l]	0.64	0.89	0.18	-94	-165/-175[i]	-183/-171[i]	-3.5	-0.70	2	8	5
Mbs(3)	1.50	0.73	0.97	-93	-155	-174	-3.5	-0.64	-4	2	-4
Mbs(10)_r3	0.72	0.88	0.23	-96	-171	-183	-3.6	-0.62	-3	5	-3
Mbmin(10)	0.72	0.89	0.22	-96	-171	-183	-4.0	-0.70	-4	7	-2
Mbplus(10)	0.75	0.89	0.25	-98	-171	-183	-2.9	-0.67	-3	9	-1
E1(3)_z1	1.27	0.64	0.71	-88(4)	-173(12)	-151(8)	-3.0	-0.69	8	-1	15
E1(5)[h]	1.07	0.70	0.50	-88(4)	-155(10)	-151(6)	-3.0	-0.79	8	-2	15
E2(3)_b1	1.72 1.56[g]	0.29	1.29	-90(6)	-163(15)	-233(10)	-2.2	-0.72	-37	-2	59
E2(11)_b2[h,i]	0.78	0.86	0.27	-92	-134/-169[j]	-237	-2.6	-0.94	15	4	20

[a]First column contains the fit identifier (see below). The number of adjustable parameters is given between parentheses; when this number is 3, the adjustable parameters are the three angles that define the conformation of the 4H (ψ, ω_{AB} and ω_{CD}, see text). When the number is between 3 and 11, in addition the H3'-C3' dipolar vectors can adjust as a group in each of the helices A, B, C and D, and similarly for the groups of H4'-C4' dipolar vectors (the final numbers are found in Table S1b). A number between 3 and 11 indicates that only a few of these extra parameters were used. When the number is between 11 and 15, in addition the angles ω_B and ω_D and θ_B and θ_D were allowed to adjust. M(3)_r1: AB and CD helices with B-DNA geometry were used and the CTTG loop as derived by Ippel et al. (reference 14). The molecular χ-tensor was calculated as the tensor sum of the base χ-tensors using an average χ_{zz} of -13 10^{-34} m^3 (Table 1a); the fit results are shown in Figure 2 and coded as r1. M(10)_r2: as in M(3)_r1 except for the extra fitting parameters, r2 is code for fit in Figure 2; M(12): as in M(3)_r1 but with 12 fitting parameters, see above. Mbs(3): as in M3_r1 except the fit was performed with base-specific values to calculate molecular χ-tensor (see Table1); this was done to test the effect of base-specific values. Mbs(10)_r3: as in M(10)_r2 but with base specific values to calculate molecular χ-tensor (see Table 1), r3 is code of fit in Figure 2. Mbmin(10): as in M(10) except χ_{zz} was increased to –10.5 10^{-34} m^3 (minus one standard deviation); this was done to test the effect of the uncertainty in χ_{zz} on the fit results. Mbplus(10): as in M(10) except that χ_{zz} was set to –15.5 10^{-34} m^3 (plus one standard deviation). E1(3)_z1: fit with AD and BC helices taken as in an experimental structure which was based on classical constraints, such as NOEs and J-couplings (reference 3), z1 code of fit in Figure 2. The structure used was close to the average of the 20 lowest energy structures. E1(5): as in E1(3) but with extra adjustment of H3'-C3' groups of dipolar vectors. E2(3)_b1: fit with AD and BC helices taken from experimental structure based on NOE and J-coupling data, b1 is the code for the fit in Figure 2. The structure chosen was closest to the average and had an inter-helix angle of ca. -70°. E2(11)_b2: as in E2(3)_b1 but additional adjustable parameters (see above), b2 code for the fit in Figure 2; the main improvement stems from the removal of small kink between the D-helix and A-helix ($\Delta\theta_D$ = -8° and $\Delta\theta_A$ = 2°).

[b] Rmsd: root-mean-square deviation of the fit.

[c] R: linear correlation coefficient of the fit; Q: the Q-value of the fit,

$$Q = \sum_i (D_{CH,i,calc} - D_{CH,i,\exp})^2 / \sum_i (D_{CH,i,\exp})^2$$ (see reference 5i)

[d] ψ, ω_{AD}, and ω_{BC} optimal values (see text for definition). The number between parentheses is the rmsd of the distribution obtained via Monte Carlo simulation. For the Monte Carlo simulation a normal error distribution was used with a standard deviation of 0.5 Hz on the experimental D_{CH} values; 100 samples were taken and for each the fit was carried out. The molecular reference axes frame is defined in the main text. To relate ω_{AD} and ω_{BC} to the molecular structure within this frame a reference vector in each helix needs to be defined. For this, the vector v_{ABCD} is defined. It points from $<C1'>_{AD}$ to $<C1'>_{BC}$, the average C1' positions of the four junction residues in the AD and BC helix. Within the AD-helix, this vector is called v_{AD} and within the BC-helix v_{BC}. The orientation of v_{ABCD}

in the x,y plane is defined by the angle the vector makes with the x-axis of the reference. This angle is called ω_{ABCD} and similarly, the angles ω_{AD} and ω_{BC} for v_{AD} and v_{BC}. The search for the optimal fit between experimental and calculated RDC always starts from the parallel orientation of the helices. In this situation, the ω angles are called $\omega_{refABCD}$, and similarly for v_{AD} and v_{BC}, ω_{refAD} (= $\omega_{refABCD}$) and ω_{refBC} (=$\omega_{refABCD}$). Subsequently, the ω-rotations of the AD and BC helices are carried out, giving $\Delta\omega_{AD}$ and $\Delta\omega_{BC}$, respectively (the ω-rotations of the AD and BC helices are around a point centered on the $<C1'>_{AD}$ and $<C1'>_{BC}$ positions, respectively). These $\Delta\omega_{AD}$ and $\Delta\omega_{BC}$ rotations affect the x,y-plane orientation of v_{AD} and v_{BC}. In the final optimal orientation, ω_{AD} and ω_{BC} are then given as $\Delta\omega_{AD} + \omega_{refAD}$ (= $\Delta\omega_{AD} + \omega_{refABCD}$) and $\Delta\omega_{BC} + \omega_{refBC}$ (= $\Delta\omega_{BC} + \omega_{refABCD}$), respectively. Hence, ω_{AD} and ω_{BC} are the angles off the x-axis of the molecular reference axes frame of the projection of v_{AD} and v_{BC} on the x,y-plane in the final optimal orientation. For the 4H with model B-DNA helices $\omega_{refABCD}$ = -170°. For the mRDC-optimized 4H with helices from experimental NOE-based 4H structures: $\omega_{refABCD}$ = -161° (E1); $\omega_{refABCD}$ = -140° (E2).

[e] χ_{ax}' and R of the optimized 4H. R is defined in the main text and χ_{ax}' equals D_{CH}^{max} and is expressed in Hz.

[f] The Euler angles defining the orientation of the molecular χ-tensor in the final optimal conformation and with respect to the defined reference axes system (see main text).

[g] The average Rmsd obtained from the Monte Carlo simulation; generally the Monte Carlo Rmsd's tend to spread in such a way that they are somewhat lower on average also for the other fits.

[h]The additional ω-rotation of the group H3'-C3' vectors and the group of H4'-C4' vectors are given in Table S1b.

[i]The fit has in addition separate ω-rotation of D- and C-helices. The numbers given are ω_A and ω_B for the A- and B-helices, respectively, the corresponding ω_D and ω_C are behind slash.

[j]The fit has in addition separate ω-rotation of helix D (ω_D behind slash).

Table S1b Optimized Δω-rotations[a] of the H3'-C3' and H4'-C4' vectors

Fit/ω	3'A[b]	4'A	3'D	4'D	3'B	4'B	3'C	4'C
M(10)_r2	40	-30	-16	0	56	36	30	-50
M(12)	40	-30	-16	0	56	36	30	-50
E1(5)	0	-60	-36	0	0	0	0	0
E2(11)_b2	30	-50	-56	8	80	40	100	-40

[a]Δω, the additional rotation of the vector compared to the starting structure;
[b]3'A stand for the group of H3'-C3' vectors in helix A etc.

Table S1c Polar angles of the junction C1'-C1' vectors in the mRDC-optimized 4H.

	8-35[a]		25-34		25-17		9-16	
	ϕ	θ	ϕ	θ	ϕ	θ	ϕ	θ
Model[b]	155	-4	154	-40	-22	-2	-57	-1
M(3)_r1	155	-16	154	-52	-16	-2	-51	-1
M(10)_r2	155	-3	151	-38	-8	-2	-43	-1
M(12)	155	-8	150	-34	-20	-2	-43	-1
Mbs(3)	154	-18	154	-54	-17	-2	-52	-1
Mbs(10)_r3	155	-3	151	-38	-8	-2	-43	-1
Mbmin(10)	155	-3	151	-38	-8	-2	-43	-1
Mbplus(10)	155	-3	150	-38	-8	-2	-43	-1
E1(3)_z1	155	10	158	-29	-57	9	-94	12
E1(5)	156	-8	153	-46	-57	9	-94	12
E2(3)_b1	154	29	155	-8	28	0	-7	0
E2(11)_b2	158	4	156	-57	32	0	-3	0
E1(0)	166	-2	155	-40	-47	9	-84	12
E2(0)	157	10	152	-28	-64	0	-99	0

[a]8-35 indicate the vector going C1' of residue 8 to C1' of residue 35 etc. ;
[b]Model indicates the C1' vectors orientations in the starting model with B-DNA helices, while E1(0) and E2(0) indicate the experimental NOE-based structures.

Table S2 J_{CH} at four different magnetic fields[a].

Bo^2 (MHz)	15.9616		25.012		36.0144		64.02					
	J (Hz)	Rmsd[b]	J (Hz)	Rmsd	J (Hz)	Rmsd	J (Hz)	Rmsd	Jo (Hz)[c]	Slope[c] (Hz/MHz^2)	D_{CH} (Hz)[d]	Rmsd (Hz)[d]
T20.H1'	170.8	1.0	170.8	0.3	171.8	2.2	172.3	0.1	170.3	0.033	1.6	0.6
T29.H1'	170.9	0.4	170.9	0.5	170.6	0.2	170.3	1.1	171.2	-0.015	-0.7	0.2
T40.H1'	168.4	0.3	168.3	0.3	167.9	0.3	169.4	0.5	168.2	0.012	0.6	0.6
T21.H1'	170.8	1.5	171.8	0.4	171.7	1.0	171.8	0.5	171.0	0.021	1.0	0.7
T13.H1'	170.3	0.9	170.6	0.1	170.3	1.4	171.0	0.5	170.1	0.011	0.5	0.2
T12.H1'	172.4	1.1	170.7	0.1	170.3	0.8	171.9	1.1	171.7	-0.011	-0.5	1.4
T32.H1'	175.2	0.4	175.8	0.7	176.5	1.1	178.1	0.1	174.2	0.064	3.0	0.1
T9.H1'	169.2	1.1	168.7	0.4	168.0	0.5	169.6	0.6	168.2	0.011	0.5	1.0
T35.H1'	168.1	1.0	168.5	0.3	167.9	1.1	168.4	0.4	168.1	0.010	0.6	0.4
T5.H1'	169.9	0.3	168.5	0.2	168.0	0.6	167.9	0.9	169.8	-0.036	-1.7	0.9
T29.H4'	152.7	0.2	153.4	0.5	153.6	0.1	154.9	0.5	152.2	0.044	2.1	0.2
T21/T13.H4'	151.9	1.1	152.8	0.2	152.7	0.1	154.5	0.5	151.2	0.049	2.3	0.4
T12/T20.H4'	153.0	0.5	153.1	0.1	153.1	0.0	154.9	0.5	152.1	0.039	1.8	0.5
T35.H4'	149.2	2.3	150.0	0.2	149.4	0.9	150.1	0.5	149.2	0.015	0.1	0.5
T5.H4'	151.3	0.5	150.1	0.8	150.3	0.4	151.0	0.4	150.5	0.001	0.0	1.0
T32.H4'	149.8	0.5	149.5	0.3	148.5	0.4	149.3	0.9	149.6	-0.011	-0.6	0.6
T9.H4'	152.8	2.4	152.0	0.4	152.9	0.5	155.5	1.4	151.0	0.064	3.1	1.3
T40.H4'	149.7	0.3	149.8	0.2	150.3	0.5	151.0	0.5	149.2	0.030	1.4	0.2
T20.H3'	158.0	1.1	156.1	0.8	156.9	0.5	156.3	1.7	157.6	-0.023	-1.1	1.2
T21.H3'	155.9	2.0	155.5	0.8	156.0	1.7	157.6	0.5	154.8	0.034	1.7	0.7
T12.H3'	157.3	1.6	156.8	1.2	155.0	0.5	157.3	0.9	156.5	0.004	0.2	1.3
T13.H3'	157.3	2.5	157.5	0.3	157.1	0.9	158.4	0.5	156.8	0.023	1.1	0.4
T29.H3'	156.3	0.3	156.1	0.3	156.1	0.7	157.3	0.5	155.7	0.016	0.7	0.5
T5.H3'	157.9	0.6	158.5	0.2	157.6	0.5	159.4	0.7	157.4	0.026	1.2	0.6
T9.H3'	154.2	0.7	153.6	1.9	154.1	0.5			154.3	-0.014	-0.7	0.5
T32.H3'	156.2	0.6	156.7	0.3	155.0	0.5	156.2	0.2	156.3	-0.006	-0.3	0.8
T35.H3'	157.5	1.2	156.5	0.3	156.9	0.5	156.9	1.1	157.3	-0.007	-0.2	0.6
T40.H3'			157.5	0.4	157.3	0.6			157.4	0.002	0.1	0.5

[a]The J_{CH} were measured at four different fields as described via the method of reference 8. [b]Rmsd of each measured J-coupling. [c] Jo: the J-coupling at Bo is zero as derived from the least-squares fit J_{CH} = slope Bo^2 + Jo. [d]D_{CH} = slope * (64.02-15.9616) and Rmsd is standard deviation in D_{CH}.